Electrical release of dopamine and levodopa mediated by amphiphilic *β*-cyclodextrins immobilized on polycrystalline gold

Giulia Foschi,[a,‡] Francesca Leonardi,[b,‡] Angela Scala,[c] Fabio Biscarini,[a] Alessandro Kovtun,[b] Andrea Liscio,[b] Antonino Mazzaglia[*,c] and Stefano Casalini[*,a]

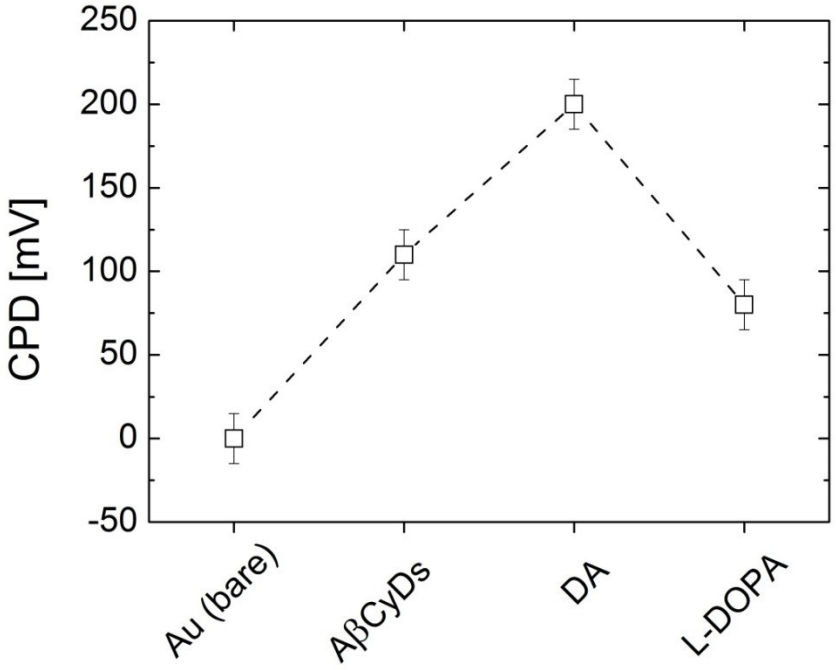

Figure S1 Contact potential difference of each functionalization step: bare Au, AβCyDs-coated Au, dopamine and L-DOPA loading.

The surface modification during each step of the functionalization protocol has been monitored by using Kelvin Probe technique (KP) In particular, KP provides a direct visualization of the surface potential modification (a.k.a. Contact Potential Difference, CPD) of the samples as shown in fig S1. For the sake of simplicity, the measured CPD values are referred to the contact potential of the bare gold surface (i.e. CP_{bare} = 0 mV). KP measurements directly provide the surface modification even if a quantitative analysis of the measured potentials is not straightforward due to the complex morphology of the AβCyD assembly. Moreover, it is noteworthy point out that the measured value corresponds to an average performed on a surface area of the sample of about 3 mm^2.

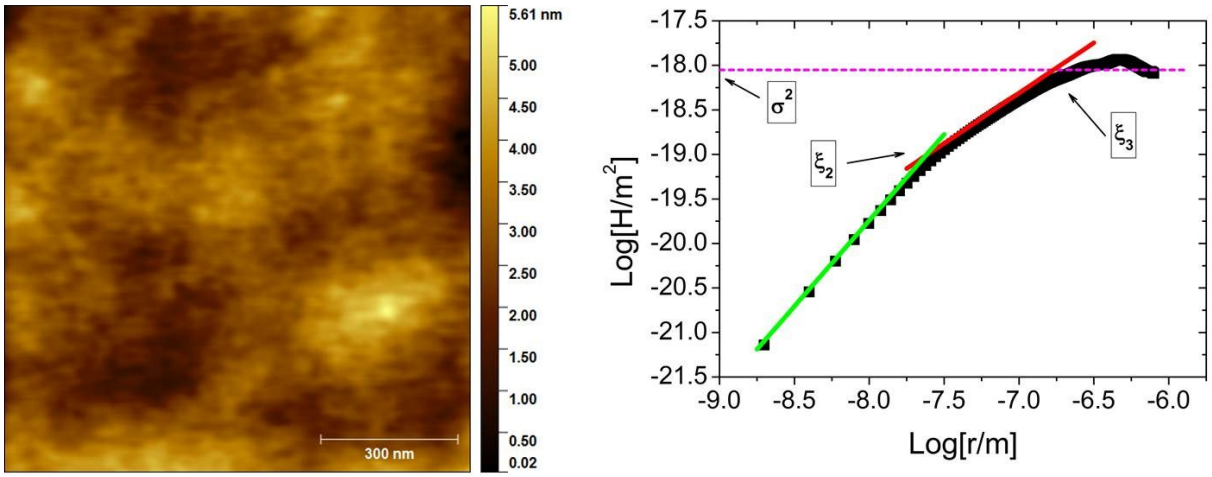

Figure S2 On the left, an AFM image (1x1 μm^2) of bare Au and on the right its height-height correlation function. Two correlation lengths are highlighted together with the roughness.

Table S1 The list of the morphological parameters for both bare and AβCyDs-coated Au

AFM parameters	AβCyDs-coated Au	Bare Au
α_1	0.11(±0.01)	-
ξ_1	3.7(±0.1)nm	-
α_2	0.60(±0.01)	0.97(±0.01)
ξ_2	18.6(±0.1)nm	24.1(±0.3)nm
α_3	0.41(±0.01)	0.57(±0.01)
ξ_3	133(±1)nm	153(±2)

As shown in Fig. S2 and Table S1, HHCF of bare Au shows only two correlation lengths and their roughness exponents, which are related to the Au atomic ordering. This analysis clearly shows that ξ_3 of AβCyDs-coated is due to the intrinsic texture of Au surface.

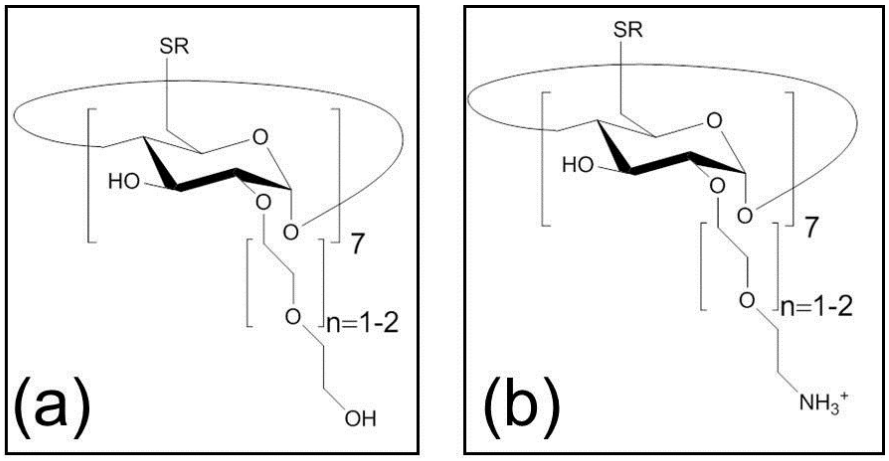

Figure S3 Chemical backbone of the two amphiphilic cyclodextrins: the amine-**(a)** and hydroxyl-terminated **(b)**.

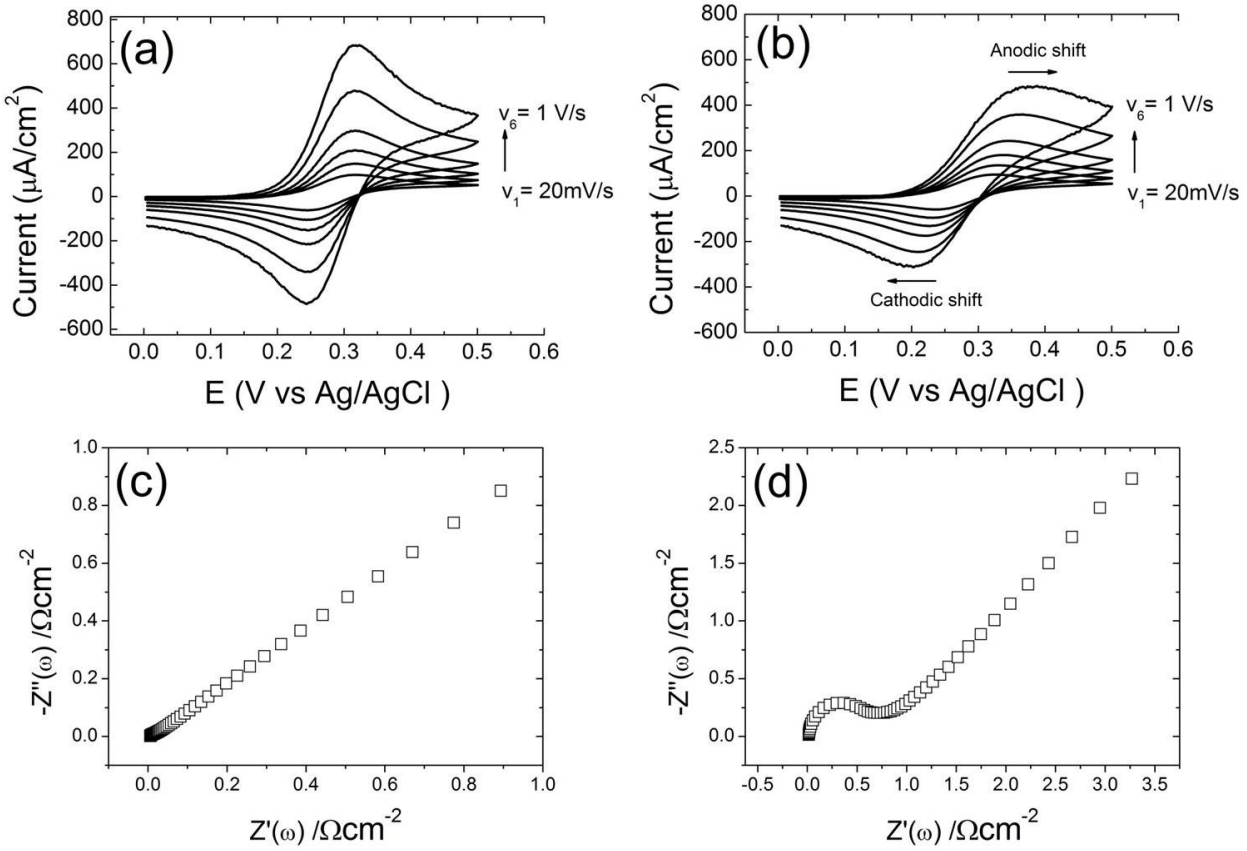

Figure S4 Overlay of cyclic voltammetries of ferricyanide probe after Au functionalization with OH- **(a)** and NH_2-terminated AβCyDs **(b)** at different scan rates, namely 20, 50, 100, 200, 500 and 1000 mV/s. Nyquist plot of Au functionalized with OH- **(c)** and NH2-terminated AβCyDs **(d)**.

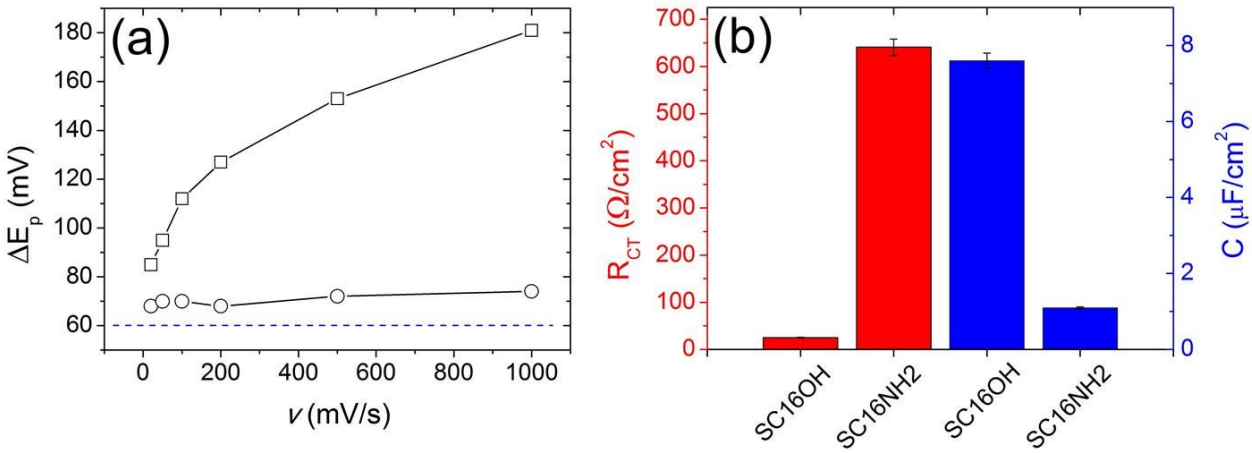

Figure S5 (a) Plot of the peak-to-peak distance (ΔE_p) as a funtion of the scan rate (v) for OH-terminated (empty circles) and NH2-terminated vesicles (empty squares). The blue dashed line stands for the ideal behavior of a reversible electron transfer reaction. **(b)** Bars overlay of charge transfer resistance (R_{CT}) in red and capacitance (C) in blue for non-ionic and cationic vesicles.

As mentioned in the main text, non-ionic vesicles cannot be immobilized onto Au electrode. Cyclic voltammetry (see Fig.S4a) and impedance spectroscopy (Fig.S4c) show the electrochemical behavior of bare Au. As a result, the electron transfer between Au and ferricyanide is reversible and no cathodic/anodic shift is observed increasing the scan rate (*i.e.* v), as shown in Fig.S5a. By comparing the impedance parameters such as charge transfer resistance (R_{CT}) and capacitance (C), the failure of non-ionic vesicles

adsorption is proved by values coherent to bare gold. On contrary, the success of cationic vesicles immobilization is demonstrated by the dramatic R_{CT} increase and consequently C decrease. Both cases show a change as high as one order of magnitude.